

Supersonic Combustion in Premixed Hydrogen-Air Flows

S. SLUTSKY,* J. TAMAGNO,† AND N. TRENTACOSTE‡
General Applied Science Laboratories, Inc., Westbury, N. Y.

This paper is concerned with the experimental determination of the over-all structure of the combustion process that takes place in a jet flow of combustible gas mixture and with the description of the mathematical procedure that has been applied successfully for analysis and prediction of the preceding experimental results. The mathematical analysis is valid for both subsonic and supersonic flows and is based upon an axisymmetric flow with diffusion, conduction, and finite-rate hydrogen-air chemistry based on phenomenological models of turbulent gas transport properties and reaction rates. New mathematical techniques of handling the finite-rate chemistry made possible fast and economical solutions of the system, using finite-difference methods. Resulting flame temperature distributions and spreading rates were computed for various values of stoichiometric equivalence ratios and showed good agreement with the experimental results. The experiments were carried out in supersonic flows because of special interest in engineering and technological applications. It was shown experimentally that a supersonic combustible mixture of hydrogen and air with temperatures far below autoignition levels may be burned in stable flame configuration without the use of any flame-holding obstructions but employing instead a small pilot flame. It was found that the stability of the resulting combustion configuration could be assured by means of pilot flames with relatively small dimensions and small total energy liberation. This technique of supersonic combustion has also been applied successfully with relatively slow reacting mixtures such as ethylene-air.

Nomenclature

c_{pi}	= specific heat of species i at constant pressure
\bar{c}_p	= specific heat of mixture at constant pressure
h_i	= enthalpy of species i per unit mass
$k_{f,s}$	= forward reaction rate
$K_{c,s}$	= equilibrium constant
Le	= Lewis number
p	= pressure
Pr	= Prandtl number
r	= normal distance to jet centerline
T	= temperature
T_0	= total temperature of stream
u	= velocity in axial direction
\dot{w}_i	= mass rate of production of species i per unit volume
W_i	= molecular weight of species
x	= axial coordinate
Y_i	= mass fraction of species i
ϵ_v	= turbulent viscosity
ν_i'	= stoichiometric coefficients for reactants
ν_i''	= stoichiometric coefficients for products
ρ	= density
ψ	= stream function as defined in Refs. 7 and 9

I. Introduction

IT is the purpose of the present report to describe some analytical and experimental work, which has been performed in order to study the feasibility of igniting a supersonic stream under conditions precluding normal spontaneous thermal ignition. Various mechanisms have been

proposed for controlling the process of combustion in high-speed ramjet engines, each of them having practical interest and with application in different speed ranges. Two fundamental mechanisms can be distinguished.

A. Combustion Control by Mass Diffusive Mixing Process

Consider a classical hypersonic ramjet engine. The engine is composed of an inlet that decelerates the air to a lower but still supersonic velocity and consequently increases the static temperature. For the high flight Mach number range (6-24) proposed for vehicles operating with this type of engine, the air at the entrance of the burner (where the fuel is added) possesses a high enough temperature to induce ignition in the fuel with which it is mixing. In most practical applications, the temperature and pressure levels in the burner are such that the reactions involved are very fast; therefore, combustion will be completed in short distances. In cases where the chemical process is considerably faster than the species diffusion process, mixing is said to be the controlling mechanism for heat release.¹

B. Combustion Control by Thermal Transport Process

In the supersonic range of flight Mach numbers, say Mach 3-6, the compression of air from ambient Mach numbers to flow conditions appropriate to the burner entrance does not increase the temperature to sufficiently high levels to insure that spontaneous thermal ignition of fuel-air mixture will occur. Some kind of external ignition source must then be utilized to initiate the reaction. If the heat produced by the local pilot reaction zone is large enough to establish a favorable balance, the reaction will proceed by heating any combustible gas mixture in the immediate vicinity and causing the flame to propagate away from its original position. The combustion rate in such a premixed flow is therefore controlled, not by the rate of diffusion of reactants, but rather by the rates of the various reactions as well as by rates of the diffusion of reaction initiators, e.g., thermally excited molecules and activated free radicals.

It must be pointed out that, in most practical applications, the two processes outlined previously for generating stable supersonic combustion will not appear perfectly independent; more likely, a combination of mass diffusion and thermal

Presented as Preprint 65-40 at the AIAA 2nd Aerospace Sciences Meeting, New York, N. Y., January 25-27, 1965; revision received April 23, 1965. The work presented here has been supported in part by the Air Force Office of Scientific Research under AF Contract No. 49(638)-991; the Air Systems Division, Wright-Patterson Air Force Base under Contract No. AF 33(657)-10463; and NASA G. C. Marshall Space Flight Center under Contract No. NAS8-2686. The authors wish to acknowledge the contributions and helpful suggestions of Antonio Ferri, Gino Moretti, and Michael Abbott.

* Assistant Director of Advanced Technology Department. Member AIAA.

† Senior Scientist. Member AIAA.

‡ Engineer; now Research Assistant Polytechnic Institute of Brooklyn.

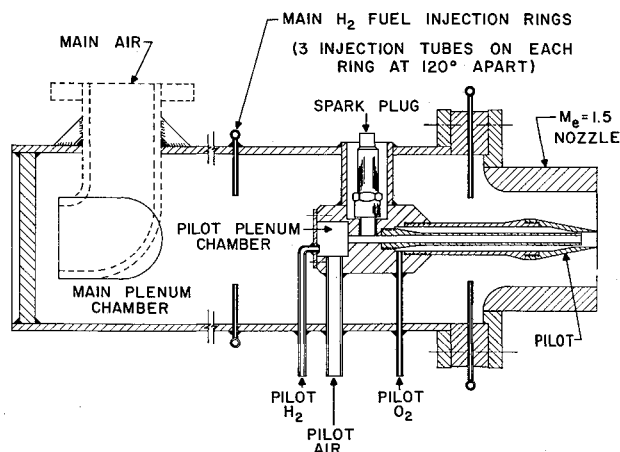


Fig. 1 Experimental apparatus.

transport will always be present. Most of the investigations and studies heretofore performed in the field of supersonic combustion involved use of the mixing process for obtaining combustion control,^{1,2} and to the authors' knowledge, no work has been reported on ignition and flame propagation for thermally controlled combustion in a supersonic flow.

As a typical model, we have considered a supersonic pre-mixed jet, of either hydrogen air or ethylene air, with initial static temperatures far below the autoignition limits and a small pilot jet of gas having a very high static temperature acting as a continuous ignition source. The pilot flame method utilized in the present study provided an effective means of ignition and flame stabilization even with slow reactions such as in ethylene-air combustion.

In parallel with the experimental phase, a numerical study was performed. The flow field associated with the process has been studied, applying an analysis developed at General Applied Science Laboratories (GASL) which is based on a finite-difference treatment of the governing equations and which has been programed for a high-speed digital computer.

II. Experimental Technique

A diagram of the experimental apparatus used for the experiments is given in Fig. 1. A large plenum chamber was used to premix air and hydrogen of different equivalence ratios. Air entered the mixing chamber through a high-pressure conduit where its mass flow was carefully metered. Hydrogen was introduced through two circular injection rings conveniently located to insure uniform mixing of the hydrogen-air combination. The hydrogen mass flow was also carefully metered to obtain a mixture of precisely defined composition.

The high velocity required in our investigation, generally on the order of 1600 fps and occasionally in excess of 2000 fps, was obtained by expansion of the combustible mixture through a supersonic axial-symmetric nozzle of a nominal exit Mach number $M_e = 1.5$ and exit diameter of 3 in. Velocities in excess of 2000 fps were obtained in one configuration by increasing the stagnation temperature of the premixed flow. An important detail of the experimental work was the development of the pilot flame device for producing stable ignition of the combustible mixture.

The usual means employed for flame stabilization involves the placement of an object in the stream in such a way as to create a subsonic wake with local recirculating flow.³ When a combustible mixture flows past and is mixed by the turbulent eddy mechanism into this region, the long dwell time promotes local combustion and becomes a source of heat to ignite fresh mixture. In this way, the recirculation of hot gases may be applied in continuously acting and self-piloting devices. However, insertion of such a flame-holding body into a supersonic flow necessarily involves strong shocks and possible choking of the main flow. In contrast, the use

of a pilot flame results in a high-temperature thermal source with minimum disturbance of the mainstream flow.

In order to introduce the pilot, there was placed within the large plenum chamber a small stainless-steel cylinder where the pilot gases were premixed. A cold hydrogen-air mixture of equivalence ratio $\phi \sim 4$ was allowed to expand in a 0.25-in. stainless-steel tube and was ignited by a spark plug. A larger stainless-steel tube was placed concentric with the 0.25-in. pilot for expansion of the main jet to $M_e = 1.5$. Oxygen was allowed to flow in the annulus formed by the concentric tubes and to mix with and burn off the excess of hydrogen. The pilot diameter used in most experiments did not exceed 0.5 in., which constituted less than 3% of the exit cross section of the 3.0-in.-diam nozzle.

The experiments were performed in an axially symmetric free-jet configuration with matching static pressures in the pilot stream, the premixed jet, and the surrounding still air. Flame propagation angles were determined by means of time exposure direct photographs, supplemented by measurements of mean total temperature total and static pressures.^{4,5} These flame-angle photographic measurements, as well as all of the measurements required for flow-rate determination, were made for a number of different fuel-air equivalence ratios.

It can be seen from typical photographs (Figs. 2a-2c) that the initial part of the flame has practically a conical surface, thereby indicating a constant value of the flame propagation angle θ . These photographs also show that the cone angle θ has a strong dependence on the mixture composition. A curve of θ vs equivalence ratio [for constant exit Mach number (Fig. 3)] shows this dependence very clearly. (Figure 3 also shows comparison with theoretical results, which will be discussed in Sec. IV.)

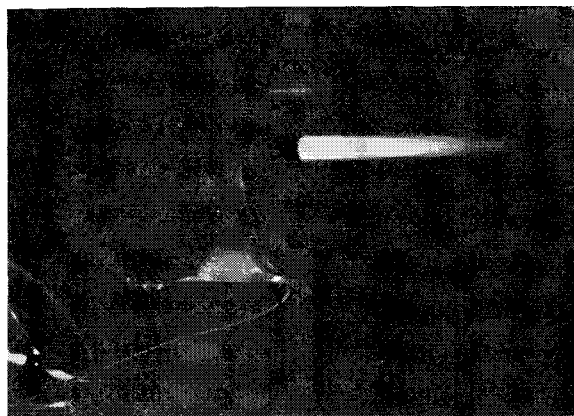


Fig. 2a Pilot and air: air Mach number, 1.47.

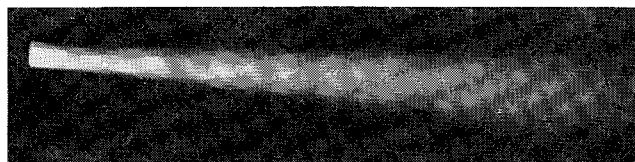


Fig. 2b Premixed H and air mixture: Mach number, 1.47
— $\phi = 0.384$.

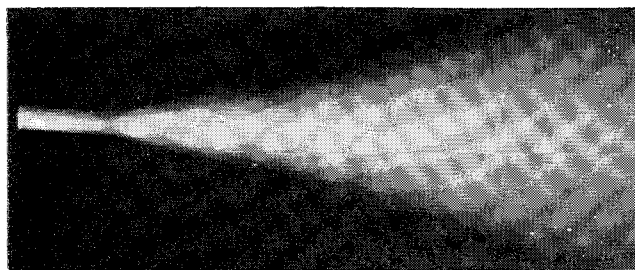


Fig. 2c Premixed H₂ and air mixture: Mach number, 1.46
— $\phi = 0.650$.

The propagation angle generally was found to be constant for a distance of approximately three nozzle diameters. Beyond this distance, the flame contour broadens more rapidly. This is explained by the fact that, beyond the three-diameter axial distance, the flame reaches a region situated outside the core of the main jet, and the influence of the mixing with the air surrounding the jet becomes important. Since the velocity in the exterior mixing region diminishes as the radial distance is increased, it is expected that the propagation angle will increase if the hydrogen diffuses out faster than the velocity, until the concentration drops below the lower combustion limit at which point the flame stops broadening.

III. Numerical Investigation of Problem

The flow field associated with the propagation of axisymmetrical flames from a pilot into a premixed hydrogen-air flow has been studied, using analytical and numerical techniques developed at GASL. These techniques depend upon two principal advances. The first involved the development of numerical "subdomain" methods of analyzing finite-rate chemical systems characterized by many components and many reactions.⁶ These numerical methods make possible the use of large finite-difference steps of unconditional stability and with resulting calculation speeds 250 times as fast as heretofore available with Runge-Kutta-based methods.

The second advance involved the coupling of the preceding numerical technique (which is essentially a one-dimensional streamline calculation) with two-dimensional and axisymmetric systems. This was carried out by dividing each species mass fraction into two components, one of which satisfied the coupled diffusion equation, whereas the other satisfied a one-dimensional coupled chemical growth equation. A stability analysis of this procedure was carried out and showed that stability was governed by the treatment of the diffusion step and was unaffected by chemistry as treated previously.⁷

The analysis includes the effect of viscosity, heat conduction, and diffusion. In general, these transfer phenomena occur as a result of both molecular action and turbulent motion, but the latter is primarily responsible in the application of interest. Boundary-layer approximations are assumed in writing the conservation laws. Since we are dealing with gases that are strongly chemically reactive, heat release by such chemical reaction is included in the energy equation. Continuity equations are satisfied for each chemical species and for the mixture. Also, the effect of energy transport by diffusion is included in the energy equation.

The equations and mechanisms governing the axisymmetric flow of a gas mixture with finite-rate reactions and diffusion are discussed in detail in Refs. 7-9. The equations used in the analysis are summarized below:

Species Continuity

$$\frac{\partial Y_i}{\partial x} = \frac{1}{\psi} \frac{\partial}{\partial \psi} \left(\frac{\epsilon_v}{Pr} Le \rho u r^2 \frac{1}{\psi} \frac{\partial Y_i}{\partial \psi} \right) + \frac{\dot{w}_i}{\rho u} \quad (1)$$

Momentum

$$\frac{\partial u}{\partial x} = -\frac{1}{\rho u} \frac{dp}{dx} + \frac{1}{\psi} \frac{\partial}{\partial \psi} \left[\frac{1}{\psi} \epsilon_v \rho u r^2 \frac{\partial u}{\partial \psi} \right] \quad (2)$$

Energy

$$\bar{c}_p \frac{\partial T}{\partial x} = \frac{1}{\rho} \frac{dp}{dx} + \frac{1}{\psi} \frac{\partial}{\partial \psi} \left[\frac{\bar{c}_p}{Pr} \frac{1}{\psi} \epsilon_v \rho u r^2 \frac{\partial T}{\partial \psi} \right] + \frac{\epsilon_v \rho u r^2}{\psi^2} \left[\left(\frac{\partial u}{\partial \psi} \right)^2 + \frac{Le}{Pr} \frac{\partial T}{\partial \psi} \sum_{i=1}^N c_{p_i} \frac{\partial Y_i}{\partial \psi} \right] - \frac{1}{\rho u} \sum_{i=1}^N h_i \dot{w}_i \quad (3)$$

where ψ is the stream function and is related to r by

$$r^2 = 2 \int_0^\psi \frac{\psi' d\psi'}{\rho u} \quad (4)$$

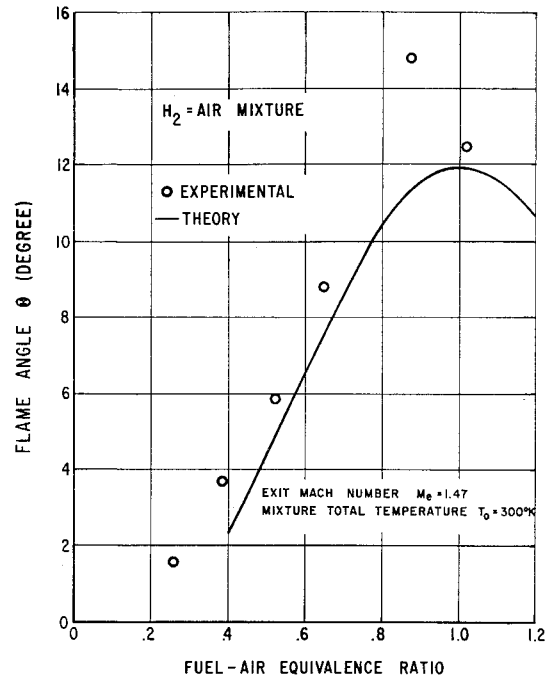


Fig. 3 Comparison between experimental and computed values of flame propagation angle.

Le is the Lewis number, Pr the Prandtl number, \bar{c}_p the mixture specific heat, and ϵ_v the viscosity. In the case of turbulent flow and transport, the turbulent equivalents of the Lewis, Prandtl, and viscous parameters must be used.

The reaction process can be described adequately by a set of R simultaneous reactions involving N distinct species of the following form:

$$\sum_{i=1}^N \nu_{i,s}' M_i \xrightleftharpoons[k_{b,s}]{k_{f,s}} \sum_{i=1}^N \nu_{i,s}'' M_i \quad \begin{cases} i = 1, 2, \dots, N \text{ (species)} \\ s = 1, 2, \dots, R \text{ (reactions)} \end{cases} \quad (5)$$

Consequently, the net mass rate of production of the species can be written as

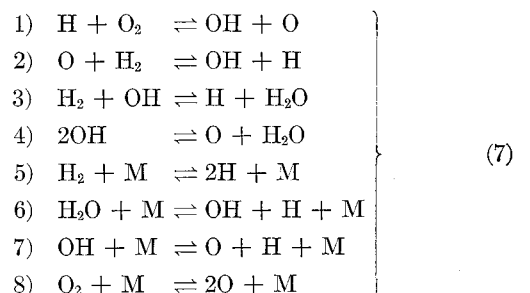
$$\dot{w}_i = W_i \sum_{s=1}^R (\nu_{i,s}'' - \nu_{i,s}') k_{f,s} \prod_{j=1}^N \left(\frac{Y_j}{W_j} \right)^{\nu_{j,s}'} \times \left[1 - \frac{\rho^{n_s}}{K_{c,s}} \prod_{j=1}^N \left(\frac{Y_j}{W_j} \right)^{\nu_{j,s}'' - \nu_{j,s}'} \right]$$

where

$$m_s = \sum_{j=1}^N \nu_{j,s}' \quad n_s = \sum_{j=1}^N (\nu_{j,s}'' - \nu_{j,s}') \quad (6)$$

and where $k_{f,s}$ = the forward reaction rate corresponding to the s chemical reaction, $K_{c,s} = k_{f,s}/k_{b,s}$ the equilibrium constant; and $k_{b,s}$ = the backward reaction rate of the chemical reactions.

The R chemical reactions taken into consideration are those described in Refs. 10 and 11 and are listed below:



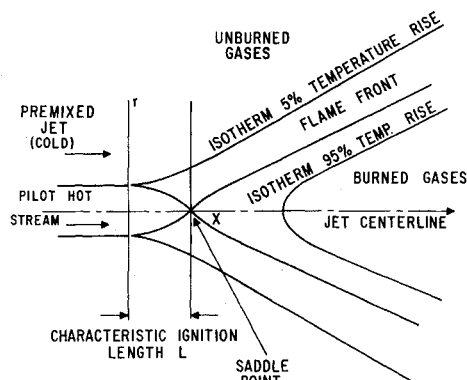


Fig. 4 Schematic representation of the flow field.

The foregoing chemical reactions involve six reacting species, although nitrogen is considered as an inert gas. The concentration of M acting as a third body is considered to be equal to the sum of all seven of the species concentration. The reaction rate coefficients used are the following:

$$\left. \begin{aligned} k_{f,1} &= 3 \times 10^{14} e^{-8810/T} \\ k_{f,2} &= 3 \times 10^{14} e^{-4030/T} \\ k_{f,3} &= 3 \times 10^{14} e^{-3020/T} \\ k_{f,4} &= 3 \times 10^{14} e^{-3020/T} \\ k_{f,5} &= 1.85 \times 10^{20} T^{-1} e^{-54,000/T} \\ k_{f,6} &= 9.66 \times 10^{21} T^{-1} e^{-62,200/T} \\ k_{f,7} &= 8 \times 10^{19} T^{-1} e^{-52,500/T} \\ k_{f,8} &= 5.8 \times 10^{19} T^{-1} e^{-60,500/T} \\ k_{b,1} &= 2.48 \times 10^{13} e^{-660/T} \\ k_{b,2} &= 1.30 \times 10^{14} e^{-2490/T} \\ k_{b,3} &= 1.33 \times 10^{15} e^{-10,950/T} \\ k_{b,4} &= 3.12 \times 10^{15} e^{-12,510/T} \\ k_{b,5} &= 10^{16} \\ k_{b,6} &= 10^{17} \\ k_{b,7} &= 10^{16} \\ k_{b,8} &= 6 \times 10^{14} \end{aligned} \right\} \quad (8)$$

T is the absolute temperature in degrees Kelvin. The rates $k_{f,1}$ – $k_{f,8}$ and $k_{b,1}$ – $k_{b,4}$ are in units $\text{cm}^3 \text{mole}^{-1} \text{sec}^{-1}$ whereas $k_{b,5}$ – $k_{b,8}$ are in $\text{cm}^6 \text{mole}^{-2} \text{sec}^{-1}$.

The detailed procedure for computing the species growth terms w_i in Eqs. (7) are discussed in Refs. 7 and 11. These procedures involve linearization of the species growth expressions, making possible the subsequent use of the subdomain method of integration of the species conservation equations instead of the usual Runge-Kutta and predictor-corrector methods.

It will be noted that a fundamental parameter in the foregoing analysis is the eddy viscosity and with it the related eddy conductivity and diffusivity. The accurate determination and fundamental specification of these quantities is the goal of a great deal of effort by many workers and is far from resolution. In order to treat practical flow problems, various phenomenological models have been devised and have been found useful in flows without combustion.^{12,13}

In order to make a first exploratory step with an order-of-magnitude estimate for the turbulent viscosity (with Lewis and Prandtl numbers of unity) use was made of the limiting downstream value $\epsilon_\infty = 3.12 \times 10^{-4} \text{ lb sec/ft}^2$ in the data of Zakkay et al.¹² This value was taken as a constant for the entire field. The resulting computing flow field is that presented in this paper.

IV. Comparison between Theory and Experiments

The results of calculations using the numerical techniques of Sec. III are presented here. Two configurations were considered analytically.

The first, simpler, model used in the theoretical analysis consists of two uniform concentric streams, one of premixed hydrogen and air and the other of the pilot gases (Fig. 4). The two streams were considered to be of equal pressure, and the pilot stream was considered to be at thermodynamic equilibrium. The velocity and temperature of the two streams were permitted to be different. In a meridional plane, generally, there is a sharp discontinuity not only in temperature but also in velocity and mass fraction in the neighborhood of the pilot. From there on, a mixing region builds involving the hot pilot gases and cold combustible mixture.

In Figs. 5a and 5b, some of the computed isotherms have been plotted and show the development of combustion. The ordinate and abscissa indicate the distances normal to and along the jet centerline, respectively.

It is seen that the external jet of combustible mixture mixes with the hot pilot gases so that the temperature of the former tends to rise, whereas the pilot stream is cooled. This process continues for a certain distance until the heat released by the reacting gases overcomes the conductive heat losses, and the temperature starts to rise along the axis. The resulting temperature distributions along the axis of symmetry are shown in Fig. 6. The point where the temperature reaches a minimum is a saddle point of the isotherm plot.

It is interesting to associate a characteristic length L with the location of this point. This length characterizes the

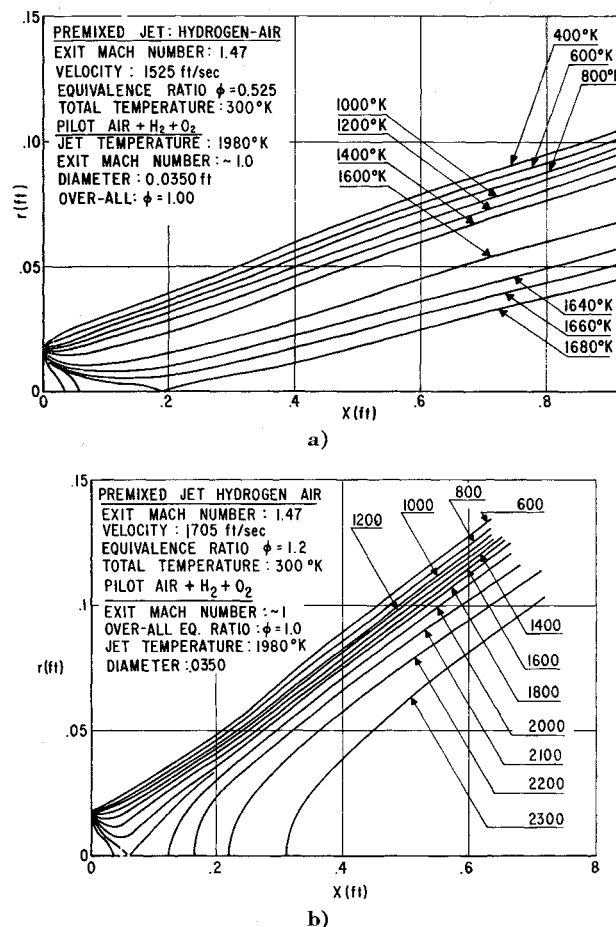


Fig. 5 Isotherms of the flow field.

extent of the zone in which the cold combustible mixtures are heated by mixing with the combustion products of the pilot; therefore, it can be considered an ignition distance. Figure 7 shows that L is dependent on the fuel-air ratio for given constant flow and geometric conditions.

Downstream of the saddle point, the isotherms start to spread out in parallel cones with a slope, which can be associated with the propagation angle mentioned before and which depends primarily on the fuel-air equivalence ratio of the premixed jet. A comparison between experimental and computed values of flame spreading angle for hydrogen-air mixtures is presented in Fig. 3. In these experiments, the total temperature and the nozzle exit Mach numbers of the premixed gases have been kept approximately constant. The results seem to indicate good agreement of the theory with experiments in this type of flame configuration.

The development of the reacting boundary separating the burned from the unburned gases (flame front) may be visualized more clearly from inspection of Figs. 8a and 8b, where constant temperature lines have been plotted as a function of the radial coordinate with increasing distance along the axis. All of the cases considered have shown nearly identical behavior. Near the initial section, and within the order of the characteristic length L where mixing is the prevailing factor, there is a tendency to smooth all of the temperature gradients. As the combustible mixture diffuses into regions, which are of high enough temperature to start the reaction, combustion products appear with associated heat release and with consequent modification of the temperature profiles. As the distance along the axis increases, the process takes on the character of a combustion wave propagating toward the cooler combustible mixture, and it is seen that after a certain distance the temperature profiles have virtually constant form but are displaced along the axial coordinate.

Figure 9a shows experimental curves of the static and total pressure. From these measurements, we conclude that the assumption of constant static pressure throughout the flow field is a good assumption.

Figure 9b shows the experimental and computed distribution of total temperature over the flame cross section. The region of maximum temperature is situated in the flame core; this is the region in which most of the combustion has already been completed. With increasing radial distance from the centerline, the temperature first decreases slowly and then drops sharply in a relatively small distance. It can be seen that the agreement between theory and experiment is excellent.

Figure 9c is a three-dimensional representation of the observed flame edge position and of the calculated static temperature at the 0.5 ft cross section. The locations of the flame edge and of the static temperature jump are in close

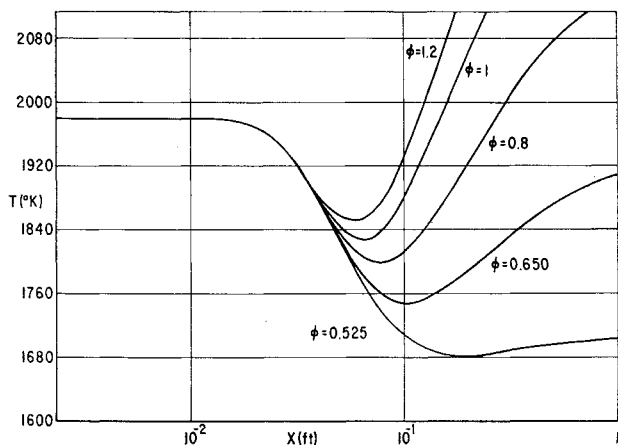


Fig. 6 Temperature distribution along the jet centerline.

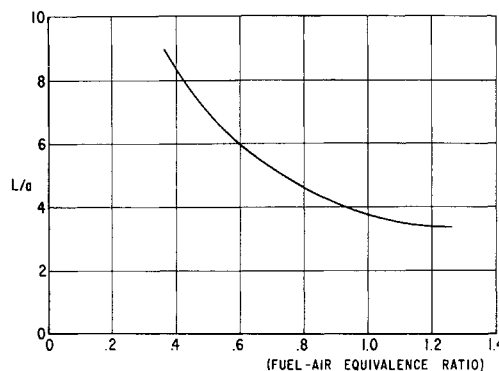


Fig. 7 Dependence of characteristic length L on fuel-air equivalence ratio: $M_e = 1.47$, mixture total temperature $T_0 = 300^\circ\text{K}$, and pilot radius $a = 0.0175$ ft.

coincidence, thereby further confirming the validity of the analysis.

An examination of the streamlines shown in Fig. 10 shows that the streamlines ahead of the flame front curve away from the axis, whereas downstream they have a tendency again to remain parallel to the axis, being straightened within the flame front. This behavior is as anticipated.

The velocity flow field, as a function of the radial distance, is presented for a typical case in Fig. 11. Typical mass fraction concentration profiles at a given cross section for the chemical species involved are presented in Fig. 12. Steep gradients denote the location of the reacting region.

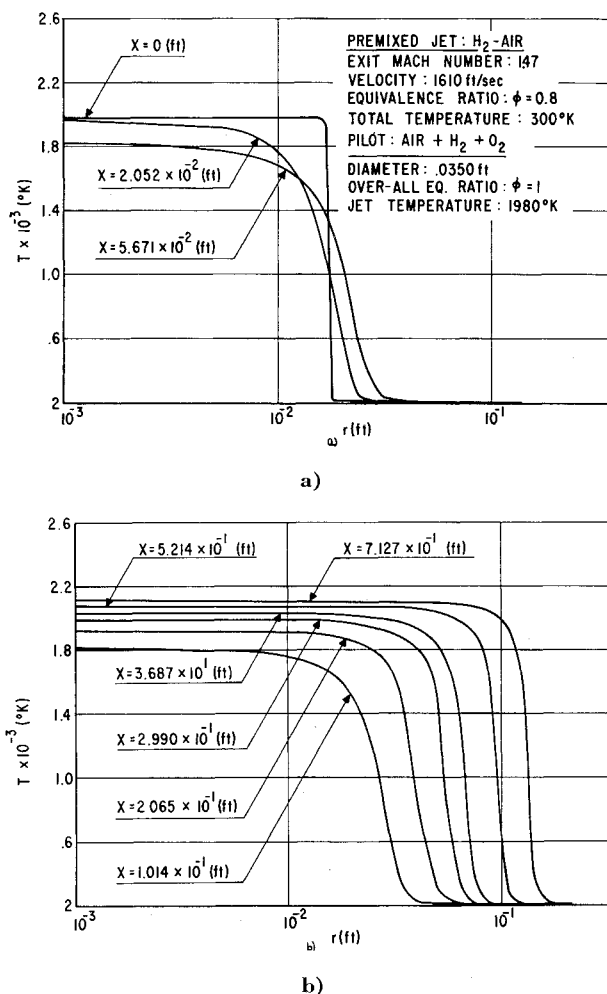


Fig. 8 Temperature distribution as a function of the normal distance to the jet centerline.

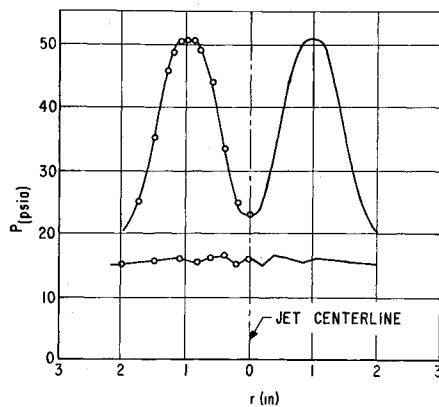


Fig. 9a Experimental static and total pressure distribution cross section 0.5 ft from exit, $\phi = 0.525$.

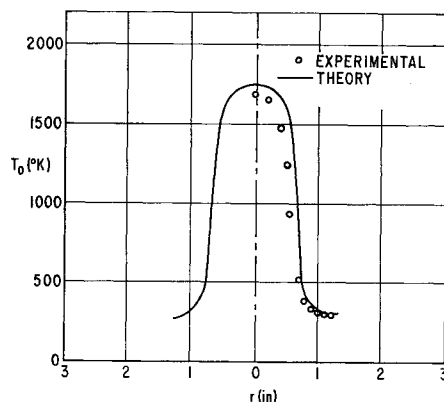


Fig. 9b Experimental and computed total temperature cross section 0.5 ft from exit, $\phi = 0.525$.

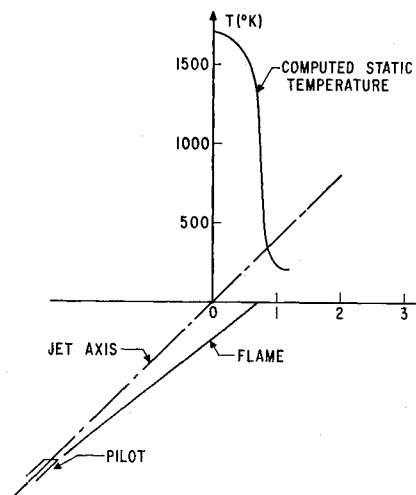


Fig. 9c Observed flame edge position and calculated static temperature.

As the distance along the axis increases, the concentration profiles develop characteristics similar to those of the temperature profiles.

As previously remarked, the preceding described model assumed the premixed hydrogen-air stream to extend radially to infinity. A second, more realistic model, was also analyzed in which the hydrogen-air stream was considered finite and bounded externally by a region of very low relative speed (100 fps). The resulting static temperature field is shown in Figs. 13a and 13b. It is seen that the initial flame behavior, including the initial combustion cone angle, is identical with that obtained from the simpler model. Subsequent

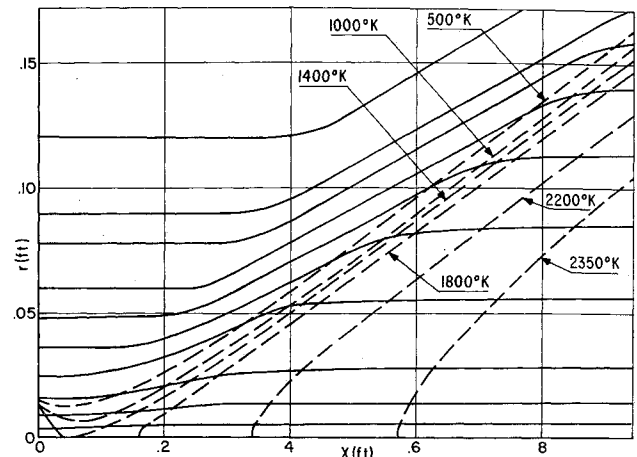


Fig. 10 Streamlines of the flow field.

behavior shows the strong effects of mixing with the external air. Thus the high-temperature contours are seen to curve back and close within a finite distance. Furthermore, it is seen that the concept of a flame front becomes unclear as a result of the increasing spread between contours, i.e., the location of the flame depends heavily upon the optical and spectral sensitivity of the photographic emulsion or other sensor with which the flame is viewed. The calculated results are in good agreement with the experiments. Photographs of the flow give good qualitative indication of the spread of the temperature contours.

For the purposes of the present numerical analysis, it was appropriate to fix a constant value of the turbulent viscosity in the entire flow field as explained in Sec. III. The success of this ad hoc procedure was remarkable, and we must ask the question why. One answer is suggested by the self-similar form of the temperature distribution in the flame front, coupled with the absence of gradients elsewhere, and the evidence gathered by many sources that the turbulence in a premixed flame front is primarily flame generated (Scurlock and Grover¹⁴ and Williams, Hottel, and Scurlock¹⁵). It is suggested that the important transport quantities here are the conductivity and diffusivity, and since the temperature and species concentration gradients propagate without change parallel to the flame front, the conductivity and diffusivity (proportional to the temperature and concentration gradient by analogy with the Prandtl mixing length hypothesis for eddy viscosity) should be unchanged along the front. Since transport is unimportant in the regions away from the flame front, a constant mean value in the neighborhood of the front should give useful results in a manner analogous to

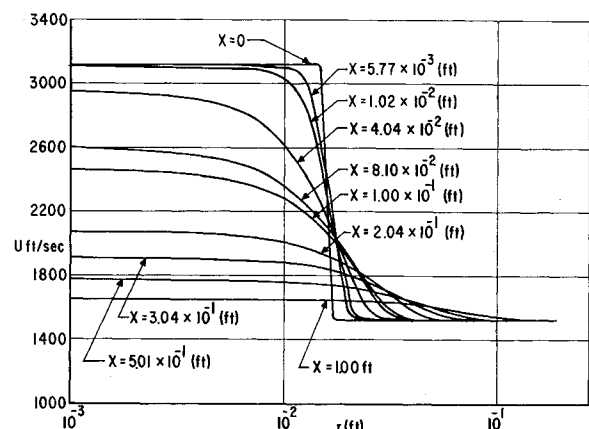


Fig. 11 Velocity flow field as a function of the normal distance to the jet centerline.

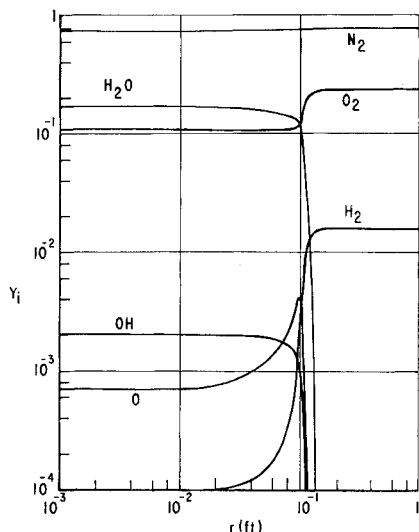


Fig. 12 Concentration profiles as a function of the normal distance to the jet centerline: $\phi = 0.525$, $X = 5.01 \times 10^{-1}$ ft.

that found for the phenomenological models for nonburning jets and wakes in which a constant value is assumed on each transverse section.

Another element of confirmation is the order-of-magnitude agreement of the value of eddy viscosity used previously and that found by others (Howe, Shipman, and Vranos¹⁶) for a somewhat similar configuration. It is reiterated here that this paper certainly makes no pretense of having eliminated the problems of mass, energy, and momentum transport and chemical kinetics in flow problems with chemical reactions, especially in turbulent flows. We are content to have solved the associated problem of coupling of transport and chemical kinetics with two-dimensional or axisymmetric flow fields and to have demonstrated the general applicability and usefulness of this analysis in flow field descriptions with combustion.

V. Conclusions

An experimental and theoretical study of the ignition and propagation of a turbulent flame front in a high-speed flow of combustible mixture has been performed. The following facts may be established as a result of this investigation:

1) A cold turbulent hydrogen-air mixture may be burned in a stable flame configuration at supersonic speeds without use of any flame-holding obstructions.

2) Ignition reliability may be assured by use of pilot flames with relatively small dimensions (occupying 3% of the area of the main flow) and small total energy liberation.

3) The method of ignition and combustion was demonstrated to work successfully with slow reactions such as ethylene-air combustion.

4) Measurements of flame temperature distribution and flame spreading rates were shown to be predicted by means of an analysis incorporating finite-rate hydrogen-air kinetics and axisymmetric diffusive flow.

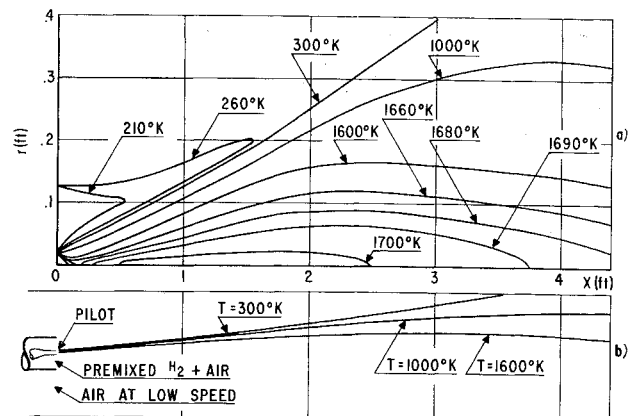


Fig. 13 Temperature field with H_2 air stream bounded externally by low-speed air.

References

- 1 Ferri, A., "Review of problems in application of supersonic combustion," *J. Roy. Aeron. Soc.* **68**, 575-597 (1964).
- 2 Zakkay, V. and Krause, E., *Mixing Problems with Chemical Reactions: Supersonic Flow, Chemical Process and Radiative Transfer*, edited by D. B. Olfe and V. Zakkay (The Macmillan Co., New York, 1964), pp. 3-29.
- 3 Phillips, D. G. and Uterberg, W., "An investigation of high speed hydrocarbon-air mixture ignition behind bluff bodies," *Pyrodynamics* **1** (January-February 1964).
- 4 Khitrin, L. M., Goldenberg, S. A., and Sunderkor, I. N., "Laws describing formation of a flame front in a free jet," NASA TT F-79 (1962).
- 5 Lewis, B. and von Elbe, G., *Combustion Flames, and Explosion of Gases* (Academic Press, New York, 1961), 2nd ed.
- 6 Crandall, S., *Engineering Analysis* (McGraw-Hill Book Co., Inc., New York, 1956), p. 147.
- 7 Ferri, A., Slutsky, S., and Moretti, L., "Mixing processes in supersonic combustion," *J. Soc. Indust. Appl. Math.* **13**, 229-258 (1965).
- 8 Pai, S. I., "Axially symmetric jet mixing of a compressible fluid," *Quart. Appl. Math.* **10**, 141-148 (July 1952).
- 9 Zeiberg, S. L. and Bleich, G. D., "Finite-difference calculation of hypersonic wakes," *AIAA J.* **2**, 1396-1402 (1964).
- 10 Pergament, H. S., "A theoretical analysis of non-equilibrium hydrogen-air reactions in flow systems," AIAA Paper 63-113 (April 1963).
- 11 Moretti, G., "A new technique for the numerical analysis of nonequilibrium flows," *AIAA J.* **3**, 223-229 (1965).
- 12 Zakkay, V., Krause, E., and Woo, S. D. L., "Turbulent transport properties for axisymmetric heterogeneous mixing," *AIAA J.* **2**, 1939-1947 (1964).
- 13 Kleinstein, G., "On the mixing of laminar and turbulent axially symmetric compressible flows," Polytechnic Institute of Brooklyn, Aerospace Lab., PIBAL Rept. 756 (February 1963).
- 14 Scurlock, A. C. and Grover, J. H., *Propagation of Turbulent Flames, Fourth Symposium (International) on Combustion* (Williams and Wilkins Co., Baltimore, Md., 1953), p. 645.
- 15 Williams, G. C., Hottel, H. C., and Scurlock, A. C., *Third Symposium on Combustion, Flame and Explosion Phenomena* (Williams and Wilkins Co., Baltimore, Md., 1949), p. 21.
- 16 Howe, N. M., Shipman, C. W., and Vranos, A., *Turbulent Mass Transfer and Rates of Combustion in Confined Turbulent Flames, Ninth Symposium (International) on Combustion* (Academic Press, Inc., New York, 1963), p. 36.